Optical absorption spectra associated with donors in a three-dimensional corner under an applied electric field

1999 J. Phys.: Condens. Matter 11 5583

(http://iopscience.iop.org/0953-8984/11/29/305)

J. Phys.: Condens. Matter **11** (1999) 5583–5591. Printed in the UK PII: S0953-8984(99)01207-2

Optical absorption spectra associated with donors in a three-dimensional corner under an applied electric field

Zhen-Yan Deng†‡§, Takayoshi Kobayashi§ and Tatsuki Ohji‡

† Korea Institute for Advanced Study, 207-43 Cheongryangri-dong, Dongdaemun-gu, Seoul 130-012, Republic of Korea
‡ Superplastic Nanoscience Laboratory, National Industrial Research Institute of Nagoya, 1-1 Hirate-cho, Kita-ku, Nagoya 462-8510, Japan
§ Department of Physics, School of Science, University of Tokyo, 7-3-1 Hongo, Bunkyo-ku, Tokyo 113, Japan

E-mail: zydeng@nirin.go.jp

Received 25 January 1999, in final form 12 May 1999

Abstract. The optical absorption spectra associated with transitions from the first valence subband to donor impurities are calculated in a three-dimensional corner under an applied electric field. It is found that there are two peaks for the absorption spectra in the corner, and the width of the absorption spectra increases with the increase in the electric field strength. The comparison between the optical absorption spectra in the corner and in a cubic quantum box shows that there is one absorption peak in the cubic quantum box, and the width of the absorption spectra in the equivalent quantum box is larger than that in the corner.

1. Introduction

The development of experimental growth techniques, such as molecular beam epitaxy (MBE) and metal–organic chemical vapour deposition (MOCVD), makes it possible to confine the electrons in one, two and all three directions (quantum wells, wires and dots). The electronic band structure and the optical properties of these low-dimensional structures and semiconductor superlattices have been attracting considerable interest recently, due to their possible wide applications in microelectronics and future laser technology [1]. The impurity states are an important factor to affect the electric-transportation and optical properties in low-dimensional semiconductor structures, which have been studied by several researchers [2–6].

A corner is a simple model for a stepped surface or V-shaped grooves in a surface. This model has been used by Lee and Antoniewicz [7, 8] to study the surface bound states and surface polaron states. In fact, step structures usually exist at the interfaces of low-dimensional semiconductor structures [9–12], which affect their optical transition spectra considerably. As we know, an electric field is a traditional tool to detect the electronic behaviour under external disturbance, and it is necessary to study the electronic structures and their related optical spectra in the corner under external fields, which is helpful to understand the related experimental spectra in low-dimensional structures. In our previous papers [13–16], the electronic and impurity states in two- and three-dimensional corner structures with and without an external electric field were investigated. It was found that the electronic and impurity state behaviour in the two- (three-) dimensional corner under external electric field is similar to that in quantum wires (dots), due to the electric field pushing the electrons towards the corner. In this paper,

0953-8984/99/295583+09$30.00

we calculate the optical absorption spectra associated with transitions from the first valence subband to donor impurities in a three-dimensional corner under an applied electric field. In section 2, a theoretical framework is outlined. Numerical results and discussion are presented in section 3.

2. Theory

The three-dimensional corner structure is the same as that in [16], an infinite barrier outside the corner is considered and an electric field $\vec{F} = (1, 1, 1)(F/\sqrt{3})$ is applied along the diagonal line of the corner. The electronic wavefunctions and levels are [16]

$$\begin{aligned}
&\Phi(\vec{r}) = N_0 Ai(\xi) Ai(\eta) Ai(\zeta) \\
&\xi = (x/d) - \lambda_l \\
&\eta = (y/d) - \lambda_m \\
&\zeta = (z/d) - \lambda_n \\
&d = [\sqrt{3}\overline{h}^2/(2m_b eF)]^{1/3}
\end{aligned} \tag{1}$$

and

$$E_{lmn} = \frac{\overline{h}^2}{2m_b d^2}(\lambda_l + \lambda_m + \lambda_n) \tag{2}$$

where N_0 is a normalization constant, m_b is the electron-band effective mass inside the corner, d is the electron characteristic length under the electric field and λ_l, λ_m and λ_n are the zero points of the Airy function $Ai(-\lambda)$ [16, 17]. The ground impurity wavefunction and binding energy are

$$\begin{aligned}
&\psi(\vec{r}) = N(\beta) Ai(\xi) Ai(\eta) Ai(\zeta) \exp(-\beta|\vec{r} - \vec{r}_0|) \\
&\xi = (x/d) - \lambda_1 \\
&\eta = (y/d) - \lambda_1 \\
&\zeta = (z/d) - \lambda_1
\end{aligned} \tag{3}$$

and

$$E_b = E_0 - \min_{\beta} \langle \psi(\vec{r}) | H(\vec{r}) | \psi(\vec{r}) \rangle \tag{4}$$

where $N(\beta)$ is the normalization constant, β is the variational parameter, $\vec{r}_0$ is the impurity position, E_0 is the ground electronic level and $H(\vec{r})$ is the impurity state Hamiltonian [16].

Figure 1 shows the possible optical transitions from the first valence subband to the donor impurities in the corner, where $\overline{h}\omega_1$ and $\overline{h}\omega_2$ represent the transition energies from the first valence subband to the bottom and top of the donor impurity levels, respectively. For an optical transition from the first valence subband to a donor level, we have for the initial and final states

$$|i\rangle = \Phi_0(\vec{r}) u_i(\vec{r}) \tag{5a}$$

$$|f\rangle = \psi(\vec{r}) u_f(\vec{r}) \tag{5b}$$

where $\Phi_0(\vec{r})$ is the wavefunction for the first valence subband, $u_i(\vec{r})$ and $u_f(\vec{r})$ are the periodic parts of the Bloch state for the initial and final states, respectively.

Taking the energy origin at the first conduction subband, we have for the energy of the initial state

$$E_i = -\varepsilon_g \tag{6}$$

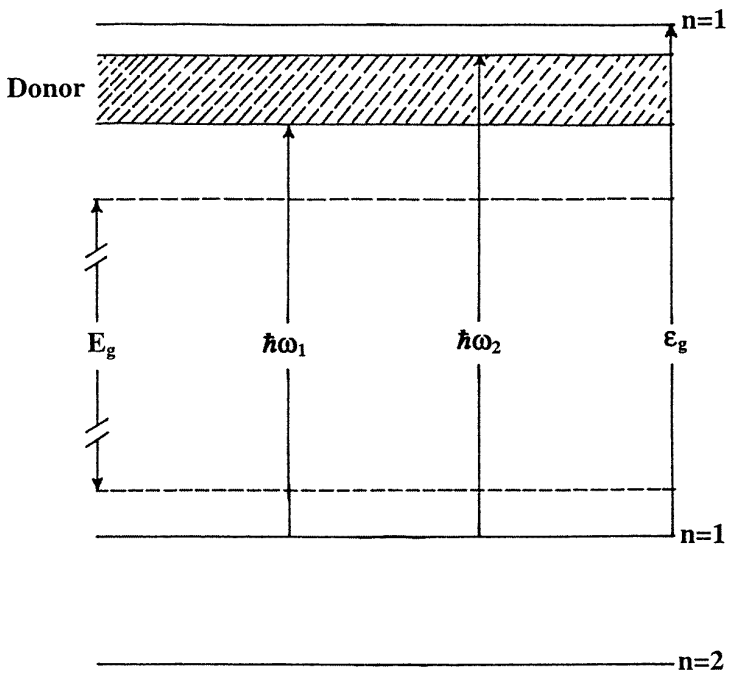

Figure 1. A schematic representation of the possible optical transitions from the first valence subband to the donor impurities in a three-dimensional corner under an applied electric field.

where

$$\varepsilon_g = E_g + E_0^c + E_0^v \tag{7}$$

with E_g being the bulk band gap and $E_0^c(E_0^v)$ the ground energy level of the first conduction (valence) subband in the corner. The energy of the final state is

$$E_f = -E_b(\vec{r}_0, F). \tag{8}$$

The transition probability per unit time for the transition from the first valence subband to the donor level associated with the impurity located at the position $\vec{r}_0$ is proportional to the square of the matrix element of the electron–photon interaction H_{int} between the wavefunctions of the initial (valence) and final (donor) state [18, 19]

$$W(\omega, F, \vec{r}_0) = \frac{2\pi}{\hbar} \sum_i |\langle f|H_{int}|i\rangle|^2 \delta(E_f - E_i - \hbar\omega) \tag{9}$$

with $H_{int} = C\vec{e} \cdot \vec{P}$, where $\vec{e}$ is the polarization vector in the direction of the electric field of the radiation, $\vec{P}$ is the electric dipole moment and C is a prefactor that describes the effect of the photon vector potential. The above matrix element may be written

$$\langle f|H_{int}|i\rangle \cong C\vec{e} \cdot \vec{P}_{fi} S_{fi} \tag{10}$$

with

$$\vec{P}_{fi} = \frac{1}{\Omega} \int_\Omega u_f^*(\vec{r}) \vec{P} u_i(\vec{r}) \, \mathrm{d}\vec{r} \tag{11}$$

and

$$S_{fi} = \int F_f^*(\vec{r}) F_i(\vec{r})\, \mathrm{d}\vec{r} \tag{12}$$

where Ω is the volume of a unit cell and $F_f(\vec{r})(F_i(\vec{r}))$ is the envelope function for the final (initial) state. Then equation (9) can be simplified further:

$$W(\omega, F, \vec{r}_0) = (2\pi/\hbar)|C|^2|\vec{e}\cdot\vec{P}_{fi}|^2|S_{fi}(\vec{r}_0)|^2 Y(\Delta) \tag{13}$$

where $Y(\Delta)$ is the step function and

$$\Delta = \hbar\omega + E_b(\vec{r}_0, F) - \varepsilon_g. \tag{14}$$

In the practical case, the implanted impurities exist everywhere in the corner. If a uniform distribution of donor impurities is considered, the total transition probability per unit time for transitions from the first valence subband to the donor impurities in the corner can be obtained:

$$\begin{aligned} W(\omega, F) &= (L_x L_y L_z)^{-1} \int_0^{L_x} \mathrm{d}x_0 \int_0^{L_y} \mathrm{d}y_0 \int_0^{L_z} \mathrm{d}z_0 W(\omega, F, \vec{r}_0) \\ &= W_0 (L_x L_y L_z)^{-1} \int_0^{L_x} \mathrm{d}x_0 \int_0^{L_y} \mathrm{d}y_0 \int_0^{L_z} \mathrm{d}z_0 \, |S_{fi}(\vec{r}_0)|^2 Y(\Delta) \end{aligned} \tag{15}$$

where

$$W_0 = (2\pi/\hbar)|C|^2|\vec{e}\cdot\vec{P}_{fi}|^2 \tag{16}$$

and $L_x \times L_y \times L_z$ is the integral zone selected in the corner. The above integrals were calculated numerically.

In order to compare the impurity state behaviour in the corner with that in quantum dots, a similar method [4, 5, 20] is adopted to calculate the impurity binding energy and optical absorption spectra in quantum dots.

3. Results and discussion

In the practical numerical calculation, a three-dimensional AlAs/GaAs corner is selected with GaAs being the well material. For simplicity, the energy is in units of effective Rydbergs, $Ryd^* = m_e e^4/(2\hbar^2\varepsilon^2)$, and the length is normalized to the effective Bohr radius, $a_0^* = \hbar^2\varepsilon/(m_e e^2)$, with m_e being the electron effective mass of the conduction band. In our calculation, we have used $\varepsilon = 12.58$, $m_e = 0.0665m_0$ and $m_h = 0.30m_0$ for the GaAs well material with m_0 being the free-electron mass and the mixing of the light- and heavy-hole bands neglected [18].

Figure 2 shows the impurity binding energy versus the impurity position along the diagonal line of the three-dimensional corner and the equivalent quantum boxes [16] for different electric fields. The equivalent side width of the cubic quantum box is $L_{eq} = \pi d/\sqrt{\lambda_1}$ and the equivalent diameter of the spherical quantum dot is $D_{eq} = 2\pi d/\sqrt{3\lambda_1}$. The results of figure 2(a) indicate that there is a peak impurity binding energy when the impurity moves along the diagonal line of the corner, and the peak impurity position becomes closer to the corner point as the electric field strength increases, which is similar to the impurity state behaviour in the quantum boxes, as shown in figure 2(b). Figure 2 also shows that the impurity binding energy in the equivalent quantum box is larger than that in the corner under the applied electric field, and the curves in figure 2(a) are asymmetrical, due to the asymmetrical confining potential of electrons in the corner.

Figure 3 shows the peak binding energy and the peak impurity position versus the electric field strength in the corner. In order to compare the difference between the corner and quantum

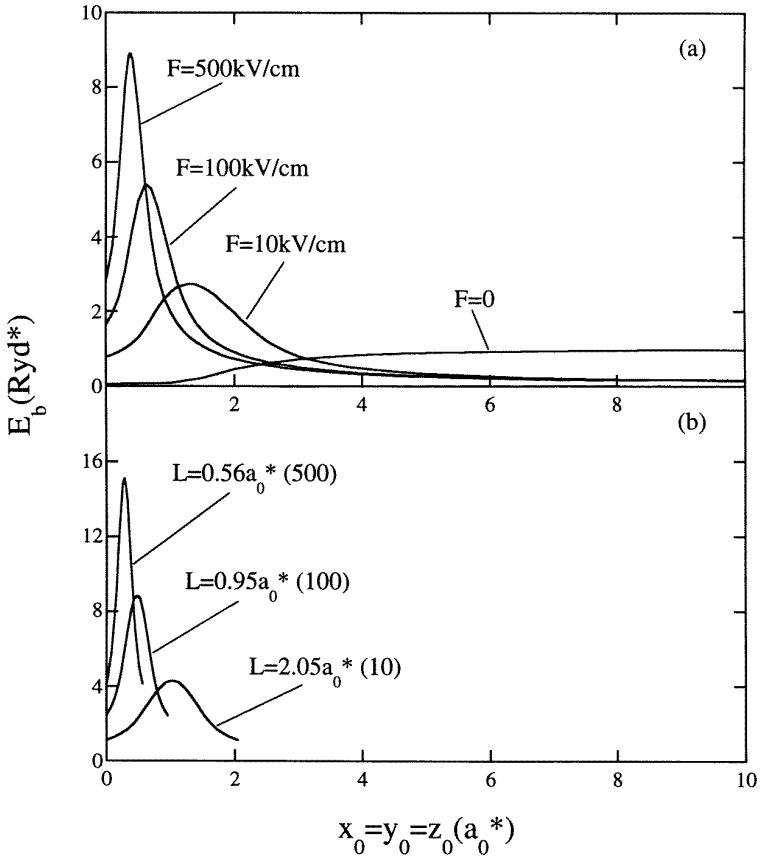

Figure 2. The dependence of impurity binding energy on the impurity position along the diagonal line of (a) the three-dimensional corner for four different electric fields, and (b) the cubic quantum box for three equivalent side widths, where the number in parentheses is the corresponding electric field strength.

dots, figure 3 also shows the maximum binding energy and its corresponding impurity position versus the dimensions (which have been changed to the equivalent electric field strength) of the cubic quantum box and the spherical dot. In fact, the peak impurity position in quantum dots is at the centre of the cubic quantum box and the spherical quantum dot, and for the spherical quantum dot, $x_0 = y_0 = z_0$ is equal to its radius. From figure 3, it can be found that the peak binding energy in the corner increases and the peak impurity position moves towards the corner point as the electric field strength increases, which are similar to the variations in peak binding energy and peak impurity position in quantum dots with their dimensions. In general, the peak binding energy in quantum dots is larger and its corresponding impurity position is smaller than those in the corner under the electric field, due to their different confining potentials. Moreover, for the same equivalent electric field strength, the maximum binding energies in the cubic quantum box and in the spherical quantum dot are almost the same, as shown in figure 3(a).

Figure 4(a) shows the optical absorption spectra associated with donors in the corner for different electric field strength. In our practical calculation, an $L_{eq} \times L_{eq} \times L_{eq}$ integral

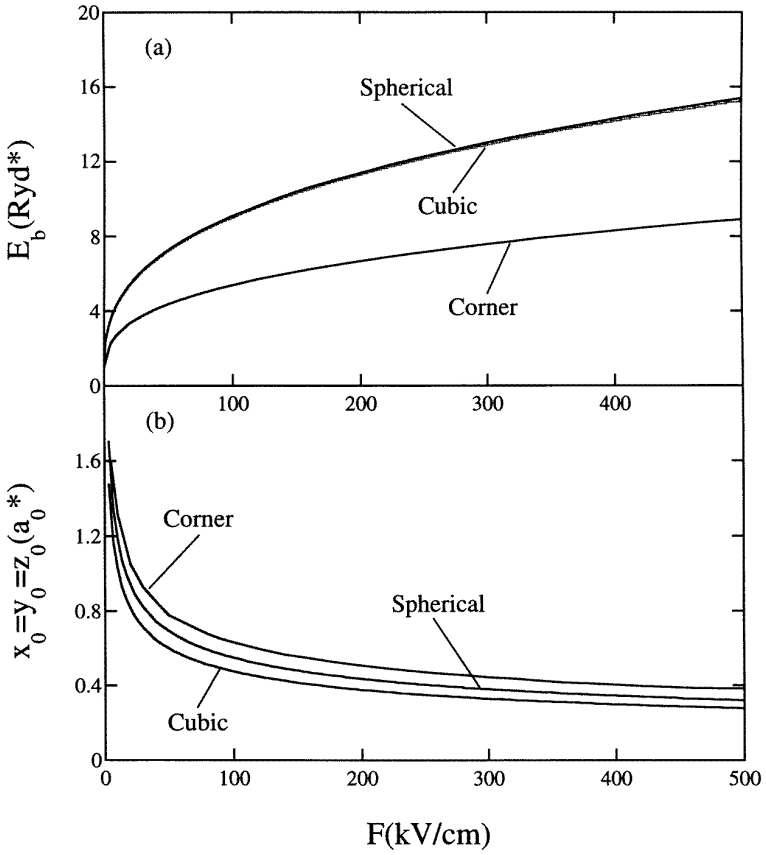

Figure 3. The dependence of (a) the maximum binding energy and (b) its corresponding impurity position in the corner and quantum dots, on the applied electric field and the dimension of quantum dots, where the diameter of the spherical quantum dot and the side width of the cubic quantum box have been transferred to the equivalent electric field strength.

zone in the corner is adopted to calculate the optical absorption spectra, which means that the donor impurities are assumed to exist only in this zone in the corner. From figure 4(a), it can be seen that there are two apparent absorption peaks on the low- and high-energy sides for the absorption spectra in the corner, and the height of the absorption peak on the low-energy side decreases as the electric field strength increases. At the same time, the width of the absorption spectra in the corner increases apparently with the increase in the electric field strength. Figure 4(b) shows the optical absorption spectra associated with donors in the cubic quantum box with different equivalent side widths, as compared with the electric field strength in figure 4(a). The results of figure 4(b) indicate that the width of the absorption spectra in the cubic quantum box increases with the decrease in its dimension, which is similar to the variation in the width of optical absorption spectra in the corner with the electric field. The difference in optical absorption spectra between the corner and the cubic quantum box is that there is no absorption peak on the low-energy side for the absorption spectra in the cubic quantum box, as compared with that in the corner, and the absorption spectra of the corner impurity levels is narrower than that of the cubic quantum box with equivalent side width.

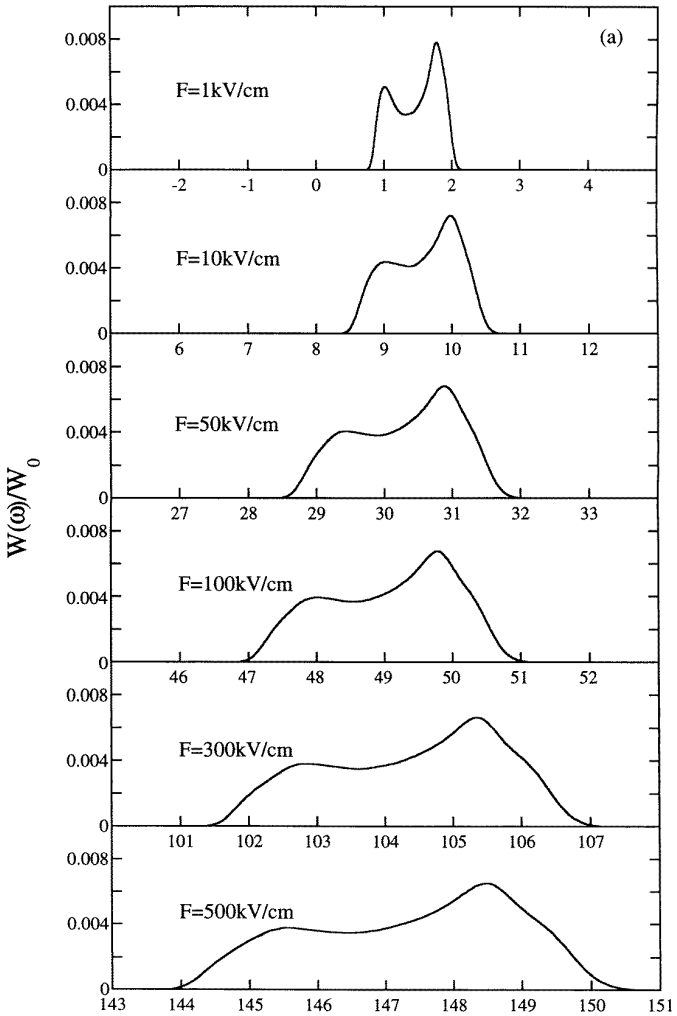

Figure 4. Optical absorption probability per unit time for the transitions from the first valence subband to the donor impurities as a function of $\hbar\omega - E_g$ (a) in the three-dimensional corner for different electric fields and (b) in cubic quantum boxes with different equivalent side widths, where the number in parentheses is the corresponding electric field strength.

As stated in our previous paper [16], because the electric field pushes the electrons towards the corner, the electrons in the well material are confined in all three directions, like the electrons confined in a quantum dot; so the electronic and impurity state behaviour in the three-dimensional corner under the electric fields are analogous to that in the quantum dots. As the electric field strength increases, the confinement of the electrons in the corner is strengthened, and the peak impurity binding energy increases. The optical absorption spectra associated with the donor impurities in the corner are related closely to the density of impurity states. Two apparent absorption peaks for the absorption spectra in the corner indicate that there are two peaks for the density of impurity states in the selected impurity distributed zone

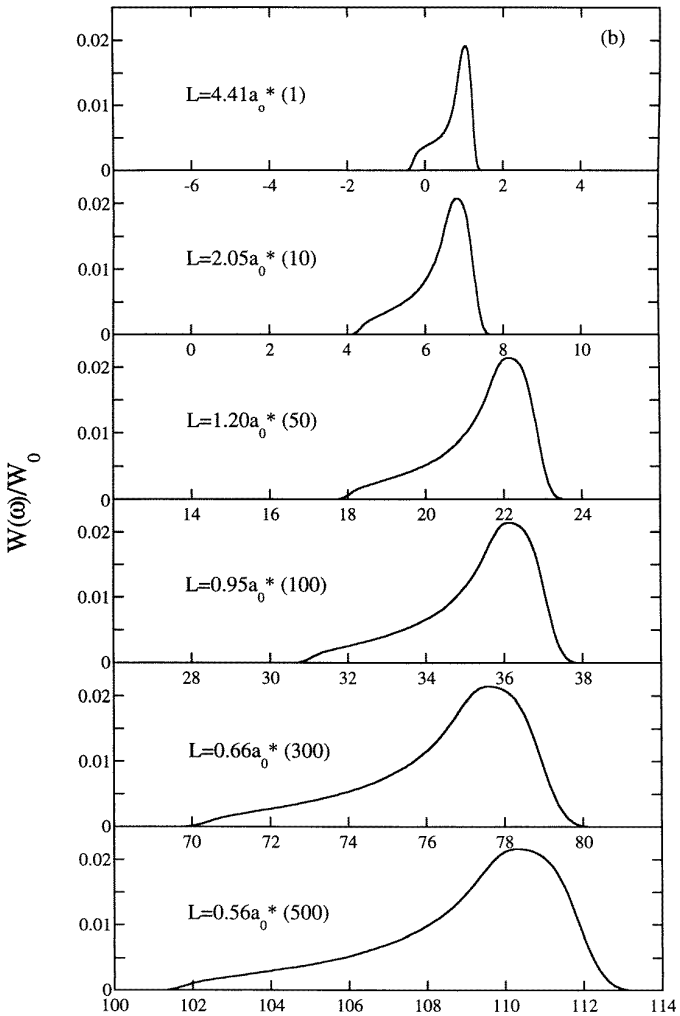

Figure 4. (Continued)

in the corner [20, 21]. The difference between the optical absorption spectra in the corner and in the equivalent quantum box may be due to the electric field induced asymmetrical electronic confining potential in the corner. The width of optical absorption spectra in the corner corresponds to the width of donor impurity levels, as shown in figure 1. When the maximum binding energy in the corner increases with the electric field, the lowest binding energy changes little, as shown in figure 2(a), and therefore the width of donor levels in the corner increases. This is the reason why the width of optical absorption spectra in the corner increases with the electric field. The same situation also happens in the cubic quantum box, as shown in figure 4(b). Because the peak binding energy in the equivalent quantum box is larger than that in the corner, as shown in figures 2 and 3, the width of the absorption spectra in the equivalent quantum box is larger than that in the corner.

In conclusion, we have studied the impurity states and their related optical absorption spectra in a three-dimensional corner under the applied electric field. It was found that the peak impurity binding energy increases with the increase in the electric field strength, and there are two apparent absorption peaks for the optical absorption spectra in the corner. The width of the absorption spectra in the corner increases as the electric field strength increases, which is analogous to the case where the width of the optical absorption spectra in the cubic quantum box increases with the decrease in its dimension.

Acknowledgments

One of the authors (Zhen-Yan Deng) would like to thank the Inoue Foundation for Science (IFS) and NEDO in Japan for support.

References

[1] Faist J, Capasso F, Sirtori C, West K W and Pfeiffer L N 1997 *Nature* **390** 589
[2] Zhu J L, Xiong J J and Gu B L 1990 *Phys. Rev.* B **41** 6001
[3] Chuu D S, Hsiao C M and Mei W N 1992 *Phys. Rev.* B **46** 3898
[4] Porras-Montenegro N and Perez-Merchancano S T 1992 *Phys. Rev.* B **46** 9780
[5] Deng Z Y, Guo J K and Lai T R 1994 *Phys. Rev.* B **50** 5736
[6] Zhu J L, Wu J, Fu R T, Chen H and Kawazoe Y 1997 *Phys. Rev.* B **55** 1673
[7] Lee W W and Antoniewicz P R 1989 *Phys. Rev.* B **40** 3352
[8] Lee W W and Antoniewicz P R 1989 *Phys. Rev.* B **40** 9920
[9] Weisbuch C, Dingle R, Gossard A C and Weigmann W 1980 *J. Vac. Sci. Technol.* **17** 1128
[10] Tanaka M and Sakaki H 1988 *Japan. J. Appl. Phys.* **27** L2025
[11] Tsuchiya M, Gaines J M, Yan R H, Simes R J, Holtz P O, Coldren L A and Petroff P M 1989 *Phys. Rev. Lett.* **62** 466
[12] Lelarge F, Wang Z Z, Cavanna A, Laruelle F and Etienne B 1997 *Europhys. Lett.* **39** 97
[13] Deng Z Y, Zhang H and Guo J K 1994 *J. Phys.: Condens. Matter* **6** 9729
[14] Zhou H Y and Deng Z Y 1997 *J. Phys.: Condens. Matter* **9** 1241
[15] Deng Z Y, Zheng Q B and Kobayashi T 1998 *J. Phys.: Condens. Matter* **10** 3977
[16] Deng Z Y, Zheng Q B and Kobayashi T 1998 *J. Phys.: Condens. Matter* **10** 2983
[17] Landau L D and Lifshitz E M 1977 *Quantum Mechanics* (Oxford: Pergamon)
[18] Porras-Montenegro N and Oliveira L E 1990 *Solid State Commun.* **76** 275
[19] Deng Z Y 1996 *J. Phys.: Condens. Matter* **8** 1511
[20] Silva-Valencia J and Porras-Montenegro N 1997 *J. Appl. Phys.* **81** 901
[21] Weber G, Schulz P A and Oliveira L E 1988 *Phys. Rev.* B **38** 2179